2023 IEEE Symposium Series on Computational Intelligence (SSCI)
Mexico City, Mexico. December 5-8, 2023

Morphological-Novelty in Modular Robot Evolution

Oliver Weissl
Vrije Universiteit Amsterdam
o.weissl@vu.nl

A.E. Eiben
Vrije Universiteit Amsterdam
a.e.eiben@vu.nl

***Abstract*—This study investigates how the introduction of morphological novelty affects the fitness and diversity of a population of modular robots. Novelty is usually measured in behavioral space, while the approach discussed in this paper assesses novelty solely using morphologies. The proposed algorithm is inspired by the histogram of oriented gradients, in combination with elements of principal component analysis, and the Wasserstein distance. The experiments conducted utilize novelty in parent selection, with different configurations. Analyzing the results, the introduction of morphological novelty promotes beneficial effects on fitness and diversity when applied correctly.**

***Index Terms*—Evolutionary Robotics, Evolvable Morphologies, Morphological Traits, Novelty Search,**

I. Introduction

Modular robots have gained significant attention in recent years because of their ability to adapt to various environments and perform a wide range of tasks. Traditional robots are often designed for a specific purpose, limiting their versatility. Modular robots on the other hand are composed of individual modules that can be connected and disconnected to form different configurations, providing greater flexibility and adaptability. However, this flexibility has a price: a very large design space where finding a good solution (i.e., a good robot configuration) is highly challenging. Evolutionary Algorithms (EA) have proved successful in solving hard optimization and design problems based on Darwinian principles of natural selection and reproduction [1]. In several cases, EAs have produced solutions that exhibit exceptional performance in their domain, defying human logic. For instance, NASA's ST5 spacecraft antenna was designed using EA, and although it lacked symmetry, it outperformed other proposed designs [2]. Humans have a bias towards symmetry, as evidenced by changes in brain activity when observing symmetrical versus asymmetrical objects [3], [4]. This bias towards symmetry can lead to good solutions being ignored or rejected because they do not conform to human schemas. Therefore, the evolution of modular robots presents an outstanding and promising opportunity. When designing robots for a specific task, evolving them with an EA can maximize performance, while avoiding human bias. However, EA can have difficulties finding a good trade-off between exploitation and exploration. Although this is a well-known topic in reinforcement learning, it is different in the context of evolutionary algorithms. The primary concern is that rapid convergence towards a particular set of traits may hinder finding potentially superior other combinations, leaving them unable to evolve. Additionally, the elements of the algorithm can exhibit biases towards specific solutions [5]. As a result, a metric should be introduced to increase the potential for exploring the fitness landscape and avoiding local maxima in agent performance [6].

In this paper, the effects of introducing morphological novelty to modular robot evolution are examined in a simulated environment, where modular robots are tasked with locomotion. To this end, we define morphological novelty by a new metric inspired by computer vision methods combined with the Wasserstein distance. This metric determines how different the morphology of a robot is from the rest of the population, and we conduct extensive experiments to compare the effect of various combinations of novelty and task performance on the evolutionary dynamics. In particular, we investigate the development of the populations' fitness and diversity as well as the evolution of specific morphological traits.

II. Related Work

Previous research on novelty in modular robot evolution defines novelty mostly based on behavior. Behavioral novelty is calculated using the sparseness around an individual's characteristics in behavioral space. This approach has been utilized in various papers, demonstrating that introducing novelty enables significant increases in population fitness due to the ability to explore new behavior [7]–[9].

Novelty, based on behavior, is also applied to research in swarm intelligence and neuroevolution. While in the domain of swarm intelligence novelty did not affect fitness significantly, the populations analyzed, exhibited more diverse behavior [10].

This characteristic, which allows for more diverse behavior, enabled Risi et al. to evolve artificial neural networks (ANNs) that significantly outperformed counterparts without novelty in a T-Maze or foraging bee problem. ANNs without novelty fell victim to deception introduced in the environments and subsequently had a slower improvement in performance [11].

For this study, the representation of genomes is crucial because it can introduce bias towards specific morphologies. For example, Miras *et al.* found that using CPPNs as genotypes favored spider-like morphologies, whereas using L-systems led to the evolution of snake-like bodies [5]. In this paper, we use L-systems to encode the morphologies.

In [12], similarly to this paper, the effects of introducing novelty on robot morphologies are investigated. The approach by Miras *et al.* uses morphological descriptors to assess novelty. Novelty is used as a selection pressure next to speed

as a fitness and a combination of fitness and novelty. Their findings suggest that using novelty as a fitness criterion enables the evolution of vastly different body structures. However, these bodies do not perform as well in terms of speed as robots whose fitness was assessed based solely on speed.

III. The Problem of Novelty

Determining novelty across a population is challenging since the essence of novelty is ambiguous. This paper only discusses the domain of morphological novelty, as novelty can also be defined through behavior [6], [8], [9]. The ambiguity of novelty arises from definitions based on human perception. What makes a morphology novel? Limbs, stationary body parts, joints, and other morphological characteristics could be used to determine novelty. Furthermore, morphological descriptors such as size and symmetry are viable for differentiating bodies. In the simulator used for this research, these concepts are composed of three essential building blocks: *bricks*, *hinges*, and the *head*. They can be translated into morphological descriptors, relying on predefined rules [13]. However, this limits the morphological novelty to the domain of the known building blocks or descriptors. When abstracting the measure of novelty from predefined concepts, new concepts, with superior performance, may arise. Having a measure that does not rely on concepts and rules that must be implemented also has the practical advantage of being universally applicable. In theory, this enables comparison across domains, which would not be possible if certain entities do not share the same building blocks or rules of substructures, such as limbs.

On another note, identical bodies that are scaled differently or rotated in space, should not be classified as different, since they are not inherently novel. The optimal measure to determine novelty would therefore be scale- and rotation-invariant while making the body more abstract to allow for a general comparison. In this study, we explore such an approach to generalize the measurement of novelty. This takes advantage of concepts used in Computer Vision, the Histogram of Oriented Gradients (HOG) combined with elements of Principal Component Analysis (PCA), and the Wasserstein Distance.

IV. Theoretical Background

A. Wasserstein Distance

The differences between probability distributions can be measured in various ways. Procedures, such as the Kullback-Leibler divergence, have significant drawbacks since they implicitly enforce symmetries that skew the measure of difference. To have a meaningful comparison between distributions, their location in probability space and their shape should be taken into account. Kantorovich and Vaserstein developed such a measure that quantifies the distance between distributions robustly. This method can be considered an approach to the optimal transport problem, in which one distribution is reshaped until it conforms to the second. The amount and distance of each perturbation influence the final distance [14], [15]. The Wasserstein distance was initially proposed for continuous space. However, for the application of measuring novelty scores, the approach is adapted for n-dimensional discrete spaces. As described in [16], the Wasserstein-1 Distance of a multi-dimensional discrete probability distribution or histogram can be described using (1), where π^* is an optimal transport plan, $c : X \times Y \Rightarrow \mathbb{R}_+$ a measure of cost and $X, Y \subset \mathbb{R}^n$ the set of locations in space, with probability measures μ, ν.

$$W_1(\mu, \nu) = \frac{\sum_{x \in X} \sum_{y \in Y} \pi^*(x, y) c(x, y)}{\sum_{x \in X} \sum_{y \in Y} \pi^*(x, y)} \tag{1}$$

For the implementation in this study, the cost function is assigned the absolute difference between points $\mu(x)$ and $\nu(y)$, with the optimal transport plan, based on the Euclidean distance between the two points.

V. Algorithm Description

A. Morphological Novelty Score

Calculating a generalizable novelty score requires the abstraction of morphologies. To achieve the necessary abstraction, the concept behind the histogram of oriented gradients (HOG) is utilized [17]. In Computer Vision HOG uses image data, giving information about the shape of its contents. The adaptation for calculating novelty is a drastic simplification of the procedure. When computing the HOG descriptors for images, the magnitude and gradient are calculated with respect to one candidate point and iterated over the entire segmented image plane. In the novelty score adaptation, the head, or the location of the brain, is considered the only candidate point. The body of each agent can be described as a set of points P in n-dimensional space, $\mathbb{R}^n; n > 2$, that is oriented around the candidate point (2). This simplification enables the translation of bodies into a standardized format (histogram) later on.

$$p - p_{head} \forall p \in P \cap p_{head} \tag{2}$$

As each morphology can have varying numbers of points in space, standardization into a uniform descriptor size is required. This is achieved by binning the points' magnitudes based on their respective rotation. The number of bins denoted as b, plays a central role as a hyperparameter for the calculation of novelty because it dictates the granularity of each descriptor. Larger bins will generalize the shape more, while smaller bin sizes allow more details. The resulting histogram has the shape depicted in (3).

$$\mathcal{H}_{\frac{360}{b}^{n-1}} \tag{3}$$

B. Rotation Invariance

To make the histograms comparable, the points P must be made rotation invariant first. Let the parts of the robot be a distribution in space, from which a covariance matrix is constructed. Applying eigendecomposition to the covariance matrix gives eigenvectors, which form the new coordinate systems basis. Where Q is the column vector of the eigenvectors,

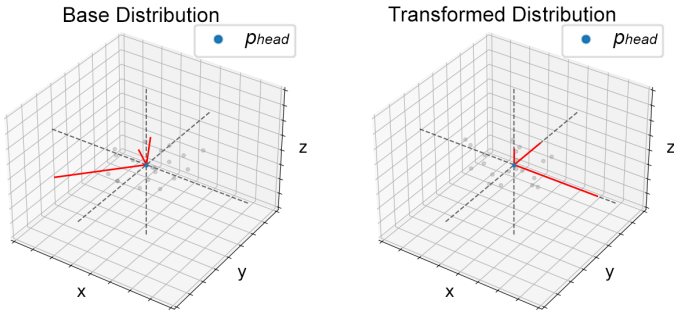

Fig. 1. Unifying Rotation by Eigenvalues

and A is a diagonal matrix of eigenvalues (4). Let $\mathcal{P}$ be the column vector of all points, with a covariance matrix $K_{\mathcal{P}\mathcal{P}}$:

$$\begin{aligned} \mathcal{P} &= P^T = [p_1, p_2, ...p_n]^T \\ K_{\mathcal{P}\mathcal{P}} &= \mathbb{E}[(\mathcal{P} - \mathbb{E}(\mathcal{P}))(\mathcal{P} - \mathbb{E}(\mathcal{P}))^T] \\ K_{\mathcal{P}\mathcal{P}} &= QAQ^{-1} \end{aligned} \tag{4}$$

The resulting eigenvectors are ranked by their respective eigenvalues, allowing for prioritized orientation in space. Change of basis is applied to all points in the grid, based on the order of eigenvalues A. Using a ranked approach to change of basis forces the n eigenvectors into the position of axes, in descending order, as seen in Fig. 1. This system of standardizing orientation is applicable for all bodies in an n-dimensional coordinate space $\mathbb{R}^n$. However, due to the simulator's robots being forced into a rigid 3D frame ($\mathbb{Z}^n$) and limited computation power, a heuristic approximation of this approach is utilized in the final implementation. The adapted approach sorts the axis by the given eigenvalues of $K_{\mathcal{P}\mathcal{P}}$, without using a change of basis on the points but switching coordinate positions.

C. Scale Invariance

Following the standardization of rotation, the final histogram is computed using the rotation and magnitude of each point to the origin (head) (5).

$$\begin{aligned} R(p) &= \begin{bmatrix} atan2(\sqrt{p_y^2 + p_z^2}, p_x)\frac{180}{\pi} \\ atan2(p_z, \sqrt{p_y^2 + p_x^2})\frac{180}{\pi} \end{bmatrix} \\ |p| &= \sqrt{p_x^2 + p_y^2 + p_z^2} \end{aligned} \tag{5}$$

Each magnitude is added to its respective bin in the histogram: $\mathcal{H}_{\lfloor \frac{R(p)}{b} \rfloor} = \mathcal{H}_{\lfloor \frac{R(p)}{b} \rfloor} + |p|$. A softmax operation is applied to the Histogram, which enforces $\sum \mathcal{H} = 1$. This step is necessary for the calculation of the Wasserstein distance, as it requires a balanced distribution [16]. Furthermore, softmax normalizes the descriptors, which finalizes the operation of making them scale-invariant.

D. Calculating Novelty

Unlike fitness, novelty is dependent on other individuals in the population. While fitness can be calculated by only considering an individual's performance, novelty requires some subset of a population to be compared with each other. Considering all Histograms of a population I, calculating novelty score using pair-wise comparison requires $\frac{|I|^2 - |I|}{2}$ novelty checks and has a time complexity of $O(n^2)$, which could be reduced by introducing neighborhood (local) novelty. The approach in this paper focuses on global comparison.

Following from (1), individuals i_{curr} novelty across the population is calculated, resulting in the populations' novelty $N(I)$. $\tilde{N}(I)$ being the normalized novelty across the populations, forcing it into range 0-1 (6).

$$\begin{aligned} n(i_{curr}) &= \sum_{i \in I \cap i_{curr}} W_1(\mathcal{H}(i_{curr}), \mathcal{H}(i)) \\ N(I) &= \{n(i)\ \forall i \in I\} \\ \tilde{N}(I) &= \{\frac{n(i)}{max(N(I))}\ \forall i \in I\} \end{aligned} \tag{6}$$

E. Applying Novelty

In order to apply novelty, the parent selection is adapted in two different ways. Selecting parents based on their fitness manifests in a convergence of a population towards some morphology or behavior [1]. The aim of this research is to counteract this convergence to allow for a better exploration of different morphologies and the fitness landscape. Fitness is the total displacement of a robot, in the measured timeframe (7). This introduction of novelty is done in the following ways:

$$f(i) = \sqrt{(i_x - i_{x\prime})^2 + (i_y - i_{y\prime})^2} \tag{7}$$

- **Weighted Novelty:** The weighted novelty selection metric is calculated in (8) where n is the novelty score, f the fitness and w the weight of novelty for an individual i. Note that for this method, the fitness should be normalized.

$$n(i) * w + f(i) * (1 - w) \tag{8}$$

- **Novelty-Fitness Product:** In contrast to the previous approach, no new parameter is introduced for determining a parent's viability (9).

$$f(i) * n(i) \tag{9}$$

VI. Experimental Setup

All experiments conducted utilized Revolve2 version v0.3.9-beta1. Available on: **github.com/ci-group/revolve2/releases**. The setup requires two changes in the *_local_runner.py* of the chosen physics engine. For this paper, the MuJoCo-based module is utilized [18].

- In the file mentioned above, the variable *env_mjcf.option.timestep* has to be lowered, in order to avoid unstable simulations (0.01 for this implementation).
- Below *for joint in posed_actor.actor.joints*, on line 345, an additional line needs to be added: *robot.find(namespace='joint', identifier=joint.name).armature = '0.2'*. This prevents unnatural vibrating behavior in the robot's joints, which

TABLE I
PARAMETERS FOR SIMULATIONS AND EVOLUTIONARY ALGORITHM

EA	*value*	*simulations*	*value*
initial mutations	10	novelty configurations	{0.0, 0.25, 0.5, 0.75, 1.0}, Prod
population size	100		
offspring size	100	parent selection	weighted novelty, novelty-fitness product
generations	400	amount of bins	20
simulation time (s)	10	seeds	1-30

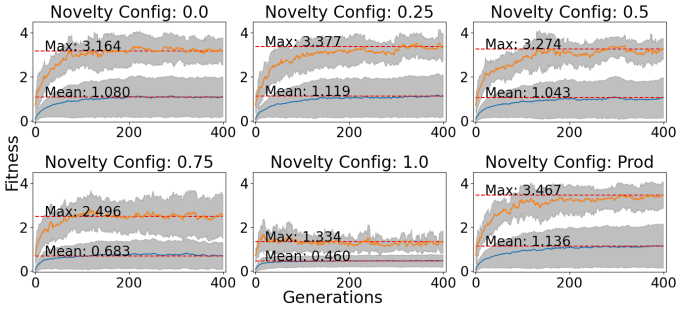

Fig. 2. Fitness Development for Novelty Configurations

are not replicable in physical robots, due to friction and servo limitations.

Table I contains parameters for all simulations. In order to describe the effects of morphological novelty, multiple configurations for the simulations are selected. In total, there are six different *novelty configurations*, which affect the extent of novelty being used for the parent selection. The two primary mechanisms for parent selection are discussed in Applying Novelty. For each configuration, 30 simulations with various seeds were performed.

VII. EXPERIMENTAL RESULTS

To investigate the population's characteristics and performances of all 180 simulations, various visualizations, and data points are utilized. Fig. 2 depicts the fitness development of all six configurations, each aggregating data from 30 different simulations. It shows the mean and max fitness values with their respective standard deviations.

To demonstrate the development of morphological novelty, a similar plot is generated using the mean novelty where additionally the minimal mean novelty is included. Refer to Fig. 3. This facilitates a better trend analysis. To display the bodies produced by different configurations, a heatmap for the last generation of each configuration is created. This plot considers the XY, XZ, and ZY-Planes and plots the frequencies of blocks appearing at a location. One limitation of this plot is assuming all building blocks are the same, preventing the investigation of the development of specific blocks as hinges or bricks. As seen in Fig. 3, the novelty score does not differ hugely for all six configurations, only three of the most significant heatmaps are shown (Fig. 4). In Fig. 5, the best five individuals from one sample simulation are presented to illustrate the effects of the novelty configurations more clearly.

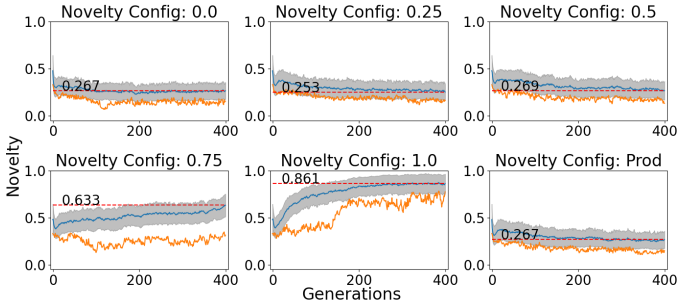

Fig. 3. Mean Novelty Development for Novelty Configurations

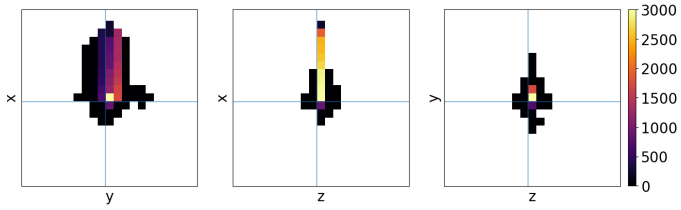

(a) 0.0 Novelty Configuration

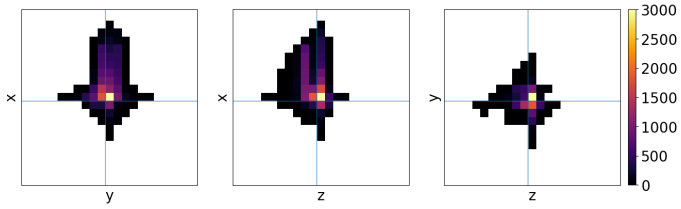

(b) 1.0 Novelty Configuration

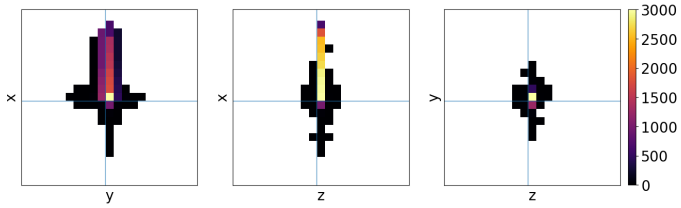

(c) Prod Novelty Configuration

Fig. 4. Average Bodies for Novelty Configurations

The data is further aggregated into a plot showing the development of novelty and fitness with respect to the novelty weight. This also allows for contextualizing the *Prod* configuration with the weighted novelty configurations. Fig. 6 illustrates the behavior of expected Fitness/Novelty depending on the novelty configuration, using a fitted curve to depict the overall trend. To facilitate better comparability of results, the morphological descriptors discussed in [13] have been evaluated for each terminal generation. For this paper, the following three morphological descriptors were selected.

1) **Coverage**: Describes the volume of the bounding box covered by the robot's modules.
2) **Limbs**: Describes the total number of parts on the morphology that can be classified as limbs with respect to the maximum possible limbs on the body.
3) **Symmetry**: Describes the symmetries of the robot's body around the head. For multi-dimensional robots, the

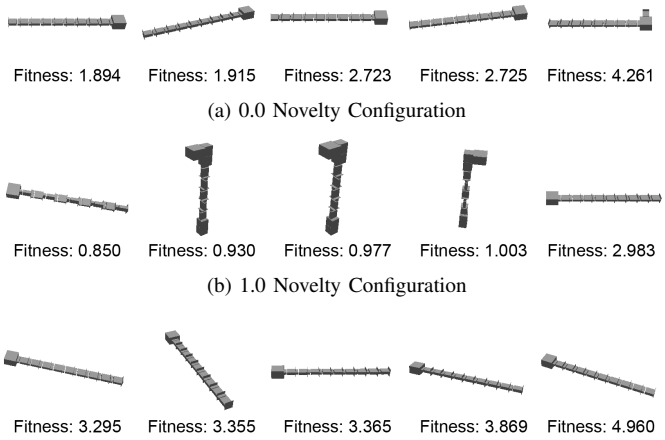

(a) 0.0 Novelty Configuration

(b) 1.0 Novelty Configuration

(c) Prod Novelty Configuration

Fig. 5. 5 Fittest Robots in One Sample Simulation

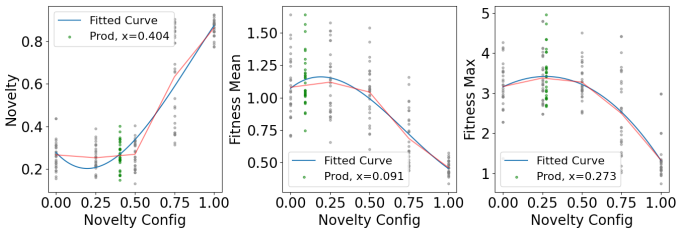

Fig. 6. Relation between Novelty Configuration and Metrics

maximum symmetry across all individual axes is used as the final value.

Coverage, number of limbs, and symmetry in Fig. 7 showcase the development of the descriptors over generations for some novelty configurations. To illustrate the variability of measures in a population, the mean standard deviation is also plotted.

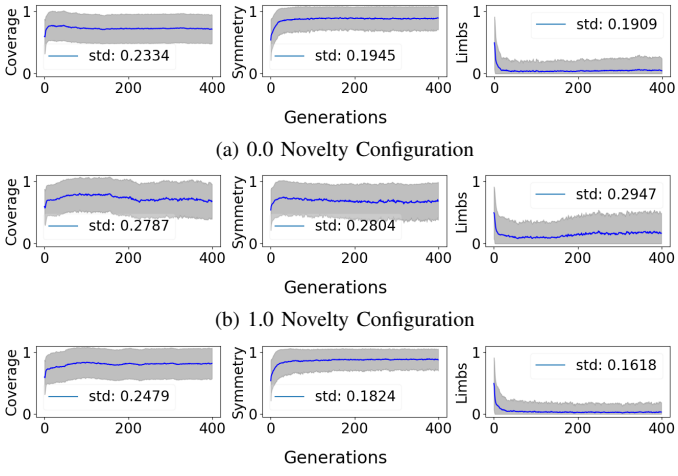

(a) 0.0 Novelty Configuration

(b) 1.0 Novelty Configuration

(c) Prod Novelty Configuration

Fig. 7. Morphological Descriptors for Novelty Configurations

TABLE II
T-TEST P-VALUES FOR NOVELTY CONFIGURATIONS

Novelty Configuration	*Fitness Mean*	*Fitness Max*	*Coverage*	*Limbs*	*Symmetry*
0.25	5.32e-01	1.90e-01	5.70e-49	9.58e-04	1.24e-02
0.5	5.26e-01	4.40e-01	7.82e-14	1.78e-02	4.18e-02
0.75	6.21e-09	3.07e-03	9.84e-01	9.05e-09	1.15e-41
1	5.32e-20	7.66e-18	2.75e-01	9.67e-11	9.04e-69
Prod	3.29e-01	6.13e-02	1.28e-62	2.75e-03	3.44e-03

VIII. Analysis and Discussion

The research question posed in this paper is: How does the introduction of a morphological novelty score affect the diversity and fitness of a population consisting of modular robots? To answer this, a statistical evaluation of the extracted fitness, novelty scores, and morphological descriptors is conducted as a complement to the previously described plots. For statistical testing, a T-test is used with a p-value of 0.05 as the threshold for statistical significance. The test is performed on the last generation of a simulation compared to the baseline *0.0* configuration, which does not introduce novelty.

With regards to diversity, a bias towards snake-like morphologies can be observed in the heatmaps Fig. 4 and the final best individuals in Fig. 5, which slowly disappears as the novelty takes a bigger weight in parent selection. This trend is supported by Fig. 3, which shows that observed novelty increases with increasing novelty weight in parent selection.

The statistical testing in Table II supports the claim that diversity tends to increase with novelty configurations compared to a population that does not depend on novelty. Looking at the morphological descriptors, there is a statistically significant difference in the vast majority when compared to the *0.0* configuration.

Interestingly the *0.25* and *Prod* configurations seem to behave similarly, also seen in Fig. 6. Other data points to assess diversity are the morphological descriptors described in the experimental results. Looking at Fig. 7a, all descriptors exhibit a stable convergence towards some value. In Fig. 7b, on the contrary, the trend seems to be more unstable, and the mean-std is higher than for the descriptors in Fig. 7a. This suggests that increasing the novelty weight allows for more exploration of morphologies, resulting in more diverse populations. Comparing the *Prod* configuration in Fig. 7c with the *0.0* and *1.0* configurations, interesting mismatches are visible. While coverage seems to behave similarly to coverage in *1.0* configurations, the symmetry and limbs descriptor seem more stable than in the *0.0* configuration.

Diversity, however, is not the singular focus of this research; therefore this development has to be put in respective to the observed fitness. Looking at Fig. 6, the relation between the fitness mean and max shows an inverse of the trend visible for novelty. Increasing novelty weight decreases the expected fitness; however, introducing moderate novelty seems to have beneficial effects. Especially the *Prod* configuration produces fitter populations in both mean and max measures compared to the baseline. The same is true for the *0.25* configuration

with a smaller magnitude. This trend is also visible in Fig. 2, showing that the *0.25* and *Prod* configurations end up with a higher average mean and max fitness in the last generation. While in Table II there is no statistical significance in the difference in fitness measure, the morphological descriptors analyzed show significant differences for those configurations. This suggests that while introducing a moderate amount of novelty does not significantly impact fitness, it changes the composition of populations.

As observed in the analysis above, the *Prod* configuration seems to have some advantages over weighted configurations. While it also is a parameterless method to use novelty, it affects a population's novelty and fitness measures differently. As seen in Fig. 6, the *Prod* configuration is put into relation with the weighted configuration based on a fitted curve. The x-value of which would be the corresponding weighted configuration. In the domain of novelty, the *Prod* configuration seems to correspond to a *0.4* weighted configuration, while in the domain of fitness, the expected weight is around *0.27* and *0.1* respectively. This suggests that using a fitness-novelty product has more impact on diversity while not having as many negative effects on fitness, offering some sort of edge over weighted configurations.

IX. Conclusion

The research question posed in this paper is how the inclusion of morphological novelty among the selection criteria affects the fitness and diversity of a population of modular robots. Diversity was measured using the proprietary novelty score, based on the algorithm discussed in this paper, in combination with morphological descriptors established in [13]. Some interesting trends have been identified in the analysis, and certain effects of novelty are clearly demonstrated. As observed in the analysis, diversity measures generally exhibit an upward trend when a higher novelty weight is enforced in the parent selection, confirming the algorithm's effectiveness in determining novelty. In contrast, fitness exhibited a downward trend when novelty was increased, as expected due to the introduction of novelty suggesting a multi-objective optimization that skews towards one objective, depending on its chosen weight. Interestingly, the analysis revealed some counterintuitive trends, showing that using a certain amount of novelty in the parent selection can enhance population performance. This effect most likely is due to the emergence of dominant morphologies, which succeed in parent selection even when their respective novelty is lower. This trend can be seen in Fig. 2-3. Furthermore, using the novelty-fitness product proved to be a favorable option. This approach exhibited a divergence in expected novelty weight based on its observed mean fitness and mean novelty. The resulting advantages make the *Prod* configuration especially useful for future research, as it is also parameterless, rendering additional optimization towards a novelty weight unnecessary.

While this paper successfully established the efficacy of the algorithm and showcased the effects of morphological novelty, there is more research to be done in this field. One particularly promising topic is neighborhood novelty, which assesses novelty on a local level, whereas the current approach does so on a global scope. Local novelty is also more aligned with potential factors in natural evolution, as evolving different behaviors or bodies, with respect to the local population, can offer survival advantages. Furthermore, the divergence observed in the penalized novelty configuration shows that novelty can be applied in many ways, potentially yielding benefits. Overall, the findings in this paper suggest numerous new areas of potential research, enabling the evolution of modular robots to more closely resemble the natural evolution of living organisms.

References

[1] A. E. Eiben and J. E. Smith, *Introduction to evolutionary computing*. Springer, 2015.

[2] G. Hornby, A. Globus, D. Linden, and J. Lohn, "Automated antenna design with evolutionary algorithms," in *Space 2006*, 2006, p. 7242.

[3] D. M. Beck, M. A. Pinsk, and S. Kastner, "Symmetry perception in humans and macaques," *Trends in cognitive sciences*, vol. 9, no. 9, pp. 405–406, 2005.

[4] M. Enquist and A. Arak, "Symmetry, beauty and evolution," *Nature*, vol. 372, no. 6502, pp. 169–172, 1994.

[5] K. Miras, "Constrained by design: Influence of genetic encodings on evolved traits of robots," *Frontiers in Robotics and AI*, vol. 8, p. 672379, 2021.

[6] J. Lehman and K. O. Stanley, "Efficiently evolving programs through the search for novelty," in *Proceedings of the 12th annual conference on Genetic and evolutionary computation*, 2010, pp. 837–844.

[7] ——, "Abandoning objectives: Evolution through the search for novelty alone," *Evolutionary Computation*, vol. 19, no. 2, pp. 189–223, June 2011.

[8] ——, "Evolving a diversity of virtual creatures through novelty search and local competition," in *Proceedings of the 13th annual conference on Genetic and evolutionary computation*, 2011, pp. 211–218.

[9] J.-B. Mouret, "Novelty-based multiobjectivization," in *New Horizons in Evolutionary Robotics: Extended Contributions from the 2009 EvoDeRob Workshop*. Springer, 2011, pp. 139–154.

[10] J. Gomes, P. Urbano, and A. L. Christensen, "Evolution of swarm robotics systems with novelty search," *Swarm Intelligence*, vol. 7, pp. 115–144, 2013.

[11] S. Risi, C. E. Hughes, and K. O. Stanley, "Evolving plastic neural networks with novelty search," *Adaptive Behavior*, vol. 18, no. 6, pp. 470–491, 2010.

[12] K. Miras, E. Haasdijk, K. Glette, and A. E. Eiben, "Effects of selection preferences on evolved robot morphologies and behaviors," in *Artificial Life Conference Proceedings*. MIT Press One Rogers Street, Cambridge, MA 02142-1209, USA journals-info ..., 2018, pp. 224–231.

[13] ——, "Search space analysis of evolvable robot morphologies," in *Applications of Evolutionary Computation: 21st International Conference, EvoApplications 2018, Parma, Italy, April 4-6, 2018, Proceedings 21*. Springer, 2018, pp. 703–718.

[14] L. V. Kantorovich, "Mathematical methods of organizing and planning production," *Management science*, vol. 6, no. 4, pp. 366–422, 1960.

[15] L. N. Vaserstein, "Markov processes over denumerable products of spaces, describing large systems of automata," *Problemy Peredachi Informatsii*, vol. 5, no. 3, pp. 64–72, 1969.

[16] G. Auricchio, F. Bassetti, S. Gualandi, and M. Veneroni, "Computing kantorovich-wasserstein distances on d-dimensional histograms using $(d+1)$-partite graphs," *Advances in Neural Information Processing Systems*, vol. 31, 2018.

[17] W. T. Freeman and M. Roth, "Orientation histograms for hand gesture recognition," in *International workshop on automatic face and gesture recognition*, vol. 12. Citeseer, 1995, pp. 296–301.

[18] E. Todorov, T. Erez, and Y. Tassa, "Mujoco: A physics engine for model-based control," in *2012 IEEE/RSJ International Conference on Intelligent Robots and Systems*. IEEE, 2012, pp. 5026–5033.